

**DIFFRACTIVE DIJET AND 3-JET ELECTROPRODUCTION
AT HERA**
(Talk presented at DIS 2000, Liverpool, April 2000)

F.-P. SCHILLING (for the H1 Collaboration)
Physikalisches Institut, University of Heidelberg, Heidelberg, Germany
e-mail: fpschill@mail.desy.de

A new H1 measurement of diffractive dijet and 3-jet production cross sections in diffractive deep inelastic scattering events of the type $ep \rightarrow eXY$ is presented. The data constrain well the diffractive gluon distribution. At low x_P , a calculation based on perturbative QCD is in a reasonable agreement with the data.

1 Introduction

At the ep collider HERA, color singlet exchange possessing vacuum quantum numbers and traditionally assessed in terms of Regge phenomenology, can be studied using a virtual photon γ^* as a probe (Fig.1a). High p_T jet production is, in contrast to inclusive F_2^D measurements, directly sensitive to the gluonic structure of diffractive exchange (Fig.1b) and enables techniques of perturbative QCD to be applied.

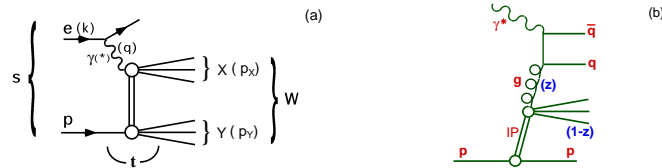


Figure 1: (a) The generic diffractive process at HERA, where a photon from the electron interacts with a proton via a net color singlet exchange, producing final state hadronic systems X and Y . Small M_X and M_Y are correlated with a large rapidity gap. (b) The dominating leading order QCD process for dijet production (BGF).

Several approaches have been developed to describe the inclusive diffractive structure function $F_2^{D(3)}(x_P, \beta, Q^2)$ as measured at HERA, including the resolved (partonic) pomeron model¹, Soft Color Interactions (SCI)^{2,3} or the Semiclassical model⁴. Two-gluon exchange models usually take the proton rest frame point of view, where the γ^* is dissociating into a $q\bar{q}$ or $q\bar{q}g$ (dominant at large M_X , i.e. low β) state, scattering elastically off the proton by the exchange of a net color singlet pair of gluons. A recent example is the Saturation model⁵, imposing a condition of strong k_T ordering on the gluon

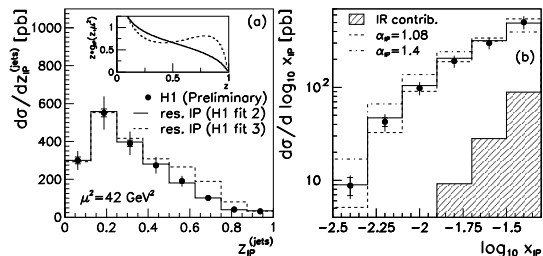


Figure 2: Diffractive dijet cross sections, compared to the resolved pomeron model.

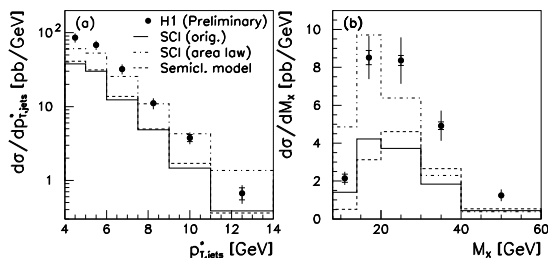


Figure 3: Dijet cross sections, compared to soft color neutralization models.

($k_{T,g} \ll k_{T,q_i}$) in the case of $q\bar{q}g$ production. The high p_T $q\bar{q}g$ configurations have also been calculated without such a condition in perturbative QCD⁶.

2 Cross Section Measurement and Results

The presented cross sections have been extracted from $\mathcal{L} = 18 \text{ pb}^{-1}$ of H1 data, using a rapidity gap selection and a cone jet algorithm with $R_{cone} = 1.0$ in the γ^*p frame. The selection yields approx. 2.500 dijet and 130 3-jet events. The kinematic range of the measurement corresponds to $4 < Q^2 < 80 \text{ GeV}^2$, $x_P < 0.05$, $|t| < 1.0 \text{ GeV}^2$, $M_Y < 1.6 \text{ GeV}$, $p_{T,jet}^* > 4 \text{ GeV}$ and $-3 < \eta_{jet}^* < 0^a$. First results, based on a sub-sample of the data, were presented in⁷.

Fig.2a presents the measured dijet cross section as a function of $z_P = \beta(1 + M_{12}^2/Q^2)$, corresponding within a partonic pomeron model to the pomeron momentum fraction entering the hard process. The prediction of the resolved (partonic) pomeron model, according to the QCD fits to $F_2^{D(3)}$ by H1⁸, is also shown. The data are well described if the “fit 2” (flat gluon) gluon density is used, whereas “fit 3” leads to an overestimate at high z_P . The corresponding

^aQuantities defined in the γ^*p frame are labeled with a “*”

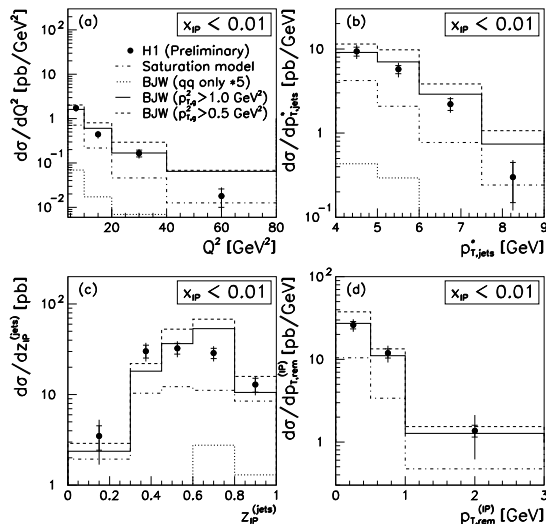


Figure 4: Dijet cross sections for $x_P < 0.01$, compared the Saturation model and the calculations by Bartels et al. (“BJW”).

gluon distributions are visualized in the insert. The dijet data constrain well the gluon distribution, in contrast to the F_2^D measurements. The x_P cross section (Fig.2b) visualizes a small Reggeon exchange contribution at high x_P . The data are consistent with a pomeron intercept value of $\alpha_P(0) = 1.2$, as obtained in ⁸. Values of 1.08 (“soft pomeron”) or 1.4 are disfavored.

Fig.3, showing cross sections differentially in the mean jet transverse momentum $p_{T,jets}^*$ and the mass of the X system M_X , demonstrates that the original ² and the area-law-improved ³ versions of SCI and the Semiclassical model fail either in shape or normalization to describe the data. However, NLO contributions have not yet been taken into account.

Fig.4 presents dijet cross sections for the restricted kinematic region of $x_P < 0.01$, avoiding the valence quark region in the proton and secondary exchange contributions. The data are compared to the Saturation model and the calculations of Bartels et al. The Saturation model, which imposes the condition $k_{T,g} \ll k_{T,q_i}$, underestimates the cross section. Within the BJW model, the contribution of $q\bar{q}$ states alone is negligible in the covered region of small β . If the p_T -cutoff for the gluon in the case of $q\bar{q}g$ production is set to $p_{T,g}^2 > 1.0 \text{ GeV}^2$, a rough agreement with the data is achieved with only one additional free parameter. Lowering this cutoff leads to an overestimate

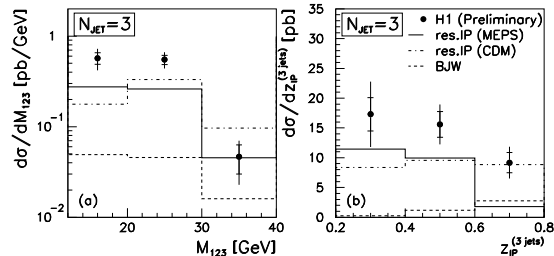


Figure 5: Diffractive 3-jet cross sections, compared to the resolved pomeron model and the two-gluon model by Bartels et al.

of the cross section, becoming visible esp. in Fig.4d, the p_T distribution of the hadronic final state not belonging to the two jets in the \mathcal{P} hemisphere.

In Fig.5, the measured 3-jet cross sections are presented as functions of the 3-jet invariant mass M_{123} and $z_{\mathcal{P}}^{(3 jets)}$, a z -variable defined for 3 jets. The partonic pomeron model, incorporating two approximations for QCD diagrams beyond leading order, the parton shower (MEPS) and color dipole (CDM) models, is below the data. The BJW two-gluon exchange calculation, well suited for 3-jet production in principle, yields too small cross sections in this phase space region, which is kinematically bound to the region of large $x_{\mathcal{P}}$.

3 Conclusions

The measurement of diffractive jet production is complementary to $F_2^{D(3)}$ measurements because it constrains well the diffractive gluon distribution. It is powerful in discriminating between different models for diffraction and can isolate perturbatively treatable contributions to $\sigma_{diff.}$ at low $x_{\mathcal{P}}$, where a reasonable agreement with a pQCD 2-gluon model is found.

References

1. G. Ingelman, P. Schlein, *Phys. Lett. B* **152**, 1985 (256).
2. A. Edin, G. Ingelman, J. Rathsmann, *Phys. Lett. B* **366**, 1996 (371).
3. J. Rathsmann, *Phys. Lett. B* **452**, 1999 (364).
4. W. Buchmüller, T. Gehrmann, A. Hebecker, *Nucl. Phys. B* **537**, 1999 (477).
5. K. Golec-Biernat, M. Wüsthoff, *Phys. Rev. D* **60**, 1999 (114023).
6. J. Bartels, H. Jung, M. Wüsthoff, *Eur. Phys. J. C* **11**, 1999 (111).
7. H1 Collaboration, paper 157ae, subm. to HEP99, Tampere (1999).
8. H1 Collaboration, T. Ahmend et al., *Z. Phys. C* **76**, 1997 (613).